



Mesomeric configuration makes polyleucine micelle an optimal nanocarrier

Journal:	<i>Biomaterials Science</i>
Manuscript ID	BM-COM-01-2016-000022.R2
Article Type:	Communication
Date Submitted by the Author:	05-Feb-2016
Complete List of Authors:	<p>He, Taoyuan; Changchun University of Technology, Department of Chemical Engineering</p> <p>Li, Di; Changchun Institute of Applied Chemistry, Key Laboratory of Polymer Ecomaterials</p> <p>Yang, Yanan; Changchun University of Technology, Department of Chemical Engineering</p> <p>Ding, Jianxun; Changchun Institute of Applied Chemistry, Key Laboratory of Polymer Ecomaterials</p> <p>Jin, Feng; Changchun Institute of Applied Chemistry, Chinese Academy of Sciences, Key Laboratory of Polymer Ecomaterials</p> <p>Zhuang, Xiuli; Changchun Institute of Applied Chemistry, Key Laboratory of Polymer Ecomaterials</p> <p>Chen, Xuesi; Changchun Institute of Applied Chemistry, Chinese Academy of Sciences, Key Laboratory of Polymer Ecomaterials</p>

Mesomeric configuration makes poly-leucine micelle an optimal nanocarrier†

Received 00th January 20xx,
Accepted 00th January 20xx

Taoyuan He,^a Di Li,^b Yanan Yang,^{*a} Jianxun Ding,^{*b} Feng Jin,^b Xiuli Zhuang^b and Xuesi Chen^b

DOI: 10.1039/x0xx00000x

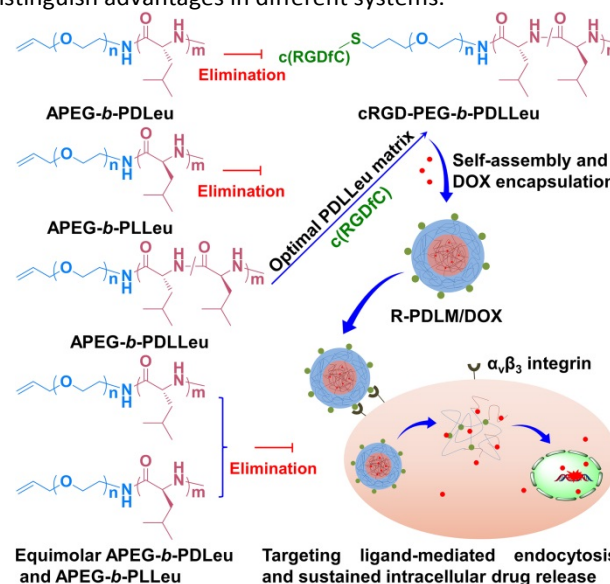
www.rsc.org/

The micelle with a mesomeric poly-leucine (PDLeu) core demonstrated the most uniform morphology, the smallest diameter, and the highest drug loading capability compared to those with dextrorotatory (PDLeu), levorotatory (PLLeu), and racemic PLLeu (PD/LLLeu) cores. In addition, the modification of c(RGDfC) endowed the optimal PDLeu micelle with enhanced intracellular drug release and cytotoxicity, indicating its great potential for targeting drug delivery.

In the past decades, the micelles from the synthetic polypeptide-composed amphiphilic block copolymers have been widely employed to controllably deliver small molecule antitumor drugs (SMADs) for synergy and attenuation.^{1,2} The sophisticated physicochemical properties of polypeptide micelles can be facilely tailored by the chemical compositions, topologies, and unique secondary structures, *e.g.*, α -helices and β -sheets, of polypeptide segments.^{3–7} Compared with other factors, the secondary structures regulated by the chiralities of contained amino acids are one kind of dexterous adjustment elements, which induce the well-defined spatial arrangements of polypeptides in micelles and determine the properties.^{4,6}

Recently, most of the previously reported polypeptide micelles for controlled drug delivery are originated from the levorotatory polypeptide segments.^{8,9} Up to now, only a few works have been reported to reveal the influence of polypeptide configurations on the properties of micelles and the release of payload.^{6,7,10,11} The obtained results indicate

that the configurations of polypeptides can dramatically adjust the properties of micelles as drug nanocarriers, and the optically active and inactive polypeptide micelles have distinguish advantages in different systems.



Scheme 1 Selection of PDLeu micelle and mechanism of targeting receptor-mediated intracellular drug delivery.

In order to systematically reveal the impact of secondary structure on the performances of polypeptide micelle, the micelles with allyloxy poly(ethylene glycol) (APEG) shell, and poly(D-leucine) (PDLeu), poly(L-leucine) (PLLeu), poly(DL-leucine) (PDLLLeu), and equimolar PDLeu and PLLeu cores were prepared, which were referred as PDM, PLM, PDLM, and PD/LM, respectively. As shown in Scheme 1, PDLM with the most uniform morphology, the smallest size, and the highest drug loading efficiency (DLE) was screened out for optimal drug delivery. Subsequently, cyclo(Arg-Gly-Asp-D-Phe-Cys) (c(RGDfC)), which can specifically recognize $\alpha_5\beta_3$ integrin overexpressed on the surface of some tumor cells (*e.g.*, human breast cancer MDA-MB-231 cells),¹² was introduced into PDLM (*i.e.*, R-PDLM) for targeting

^aDepartment of Chemical Engineering, Changchun University of Technology, Changchun 130012, P. R. China. Email: yanan@ccut.edu.cn

^bKey Laboratory of Polymer Ecomaterials, Changchun Institute of Applied Chemistry, Chinese Academy of Sciences, Changchun 130022, P. R. China. Email: jxding@ciac.ac.cn

†Electronic Supplementary Information (ESI) available: materials and methods, properties of micelles (Table S1), characterizations of copolymers (Figs. S1 and S2), stability of micelles (Fig. S3), semi-quantitative analyses of flow cytometry results (Fig. S4), and cytocompatibility of micelles (Fig. S5). See DOI: 10.1039/x0xx00000x

ligand-mediated cellular uptake and sustained intracellular drug delivery. The findings showed that the selected cRGD-decorated PDLM had great potential as a targeting nanocarrier in the advanced chemotherapy.

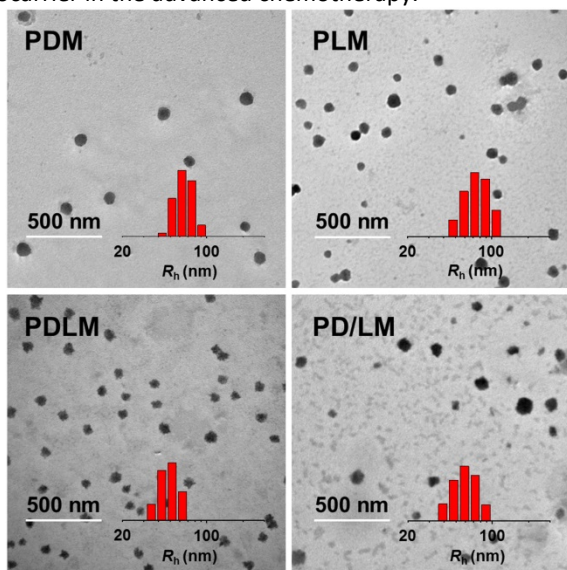


Fig. 1 Typical TEM micrographs and R_h s (insets) of PDM, PLM, PDLM, and PD/LM.

The polypeptide block copolymers can be synthesized by the ring-opening polymerization (ROP) of amino acid *N*-carboxyanhydrides (NCA) initiated by the macromolecules with one or more amino groups.¹³ In this work, we firstly synthesized APEG-*b*-PDLeu, APEG-*b*-PLLeu, and APEG-*b*-PDLLeu by the ROP of D-Leu NCA, L-Leu NCA, and equivalent D-Leu NCA and L-Leu NCA, respectively, with amino-terminated APEG (APEG-NH₂) as a macroinitiator (Scheme S1, ESI[†]). The chemical structures of obtained copolymers were demonstrated by proton nuclear magnetic resonance (¹H NMR; Fig. S1, ESI[†]) and Fourier transform infrared (FT-IR) spectra (Fig. S2, ESI[†]). As shown in Fig. S1, ESI[†], ¹H NMR spectra indicated the resonance signals at 5.3 and 5.9 ppm assigned to the protons in the double bond of allyloxy group (CH₂=CHCH₂O-), and the peak at 4.7 ppm attributed to the proton in the backbone of PLeu (-C(O)CH(CH₂CH(CH₃)₂)NH-), the signal at 3.8 ppm ascribed to the methylene protons of APEG (-CH₂CH₂O-), the peaks at 1.7 and 1.6 ppm attributed to the methylene and methine protons in the side chain of PLeu (-CH₂CH(CH₃)₂-), and the chemical shift at 0.9 ppm assigned to the methyl protons of PLeu (-CH₂CH(CH₃)₂-), which all demonstrated the successful syntheses of APEG-*b*-PDLeu, APEG-*b*-PLLeu, and APEG-*b*-PDLLeu. The degrees of polymerization (DPs) of PLeu in APEG-*b*-PDLeu, APEG-*b*-PLLeu, and APEG-*b*-PDLLeu were all calculated to be 10 by the area ratios of peaks at 4.7 and 3.8 ppm. For FT-IR spectra (Fig. S2, ESI[†]), the results also confirmed the generation of PLeu block from the appearance of the typical amide I and II bands at 1657 cm⁻¹ (ν_{C=O}) and 1547 cm⁻¹ (ν_{C(O)=NH}), respectively. In addition, c(RGDfC) was linked to the terminal of APEG-*b*-PDLLeu through thiol-ene click reaction (Schemes 1 and S1, ESI[†]). The complete

disappearance of the chemical shift of alkenyl protons in APEG (CH₂=CHCH₂O-) at 5.9 ppm and the new peak of 7.25 ppm demonstrated the successful synthesis of cRGD-PEG-*b*-PDLLeu (Fig. S1D, ESI[†]).

The amphiphilic polypeptide block copolymers can spontaneously self-assemble into micelles in PBS at pH 7.4.¹⁴ As shown in Fig. 1, the formed micelles, that is, PDM, PLM, PDLM, and PD/LM displayed spherical morphology, and the average diameters were 80, 72, 55, and 60 nm, respectively, measured from transmission electron microscopy (TEM) micrographs. It should be noted that PDLM with mesomeric PLeu core exhibited the most homogeneous distribution compared with the micelles with optically active and racemic PLeu. Moreover, the hydrodynamic radii (R_h s) of micelles were detected to be 66.5 ± 5.8, 70.5 ± 6.0, 52.9 ± 3.3, and 59.4 ± 5.8 nm, respectively, by dynamic laser scattering (DLS), which were depicted in the insets of Fig. 1 and listed in Table S1, ESI[†]. It is obvious that the micellar sizes determined by TEM were smaller than those by DLS, which should be mainly assigned to the systole and dehydration of micelles during the preparations of TEM specimens. The α-helical secondary conformation of the PDLeu and PLLeu blocks in APEG-*b*-PDLeu and APEG-*b*-PLLeu, respectively, conferred the hydrophobic moiety with rigidity and endowed the micelles with larger diameters in relation to PDLM and PD/LM that possessed a random coil PDLLeu and complex PD/LLeu cores.^{4, 7} It is noteworthy that PDLM exhibited the densest core in addition to the most uniform morphology compared with PDM, PLM, and PD/LM. Moreover, all these micelles demonstrated nearly constant R_h s during the incubation in PBS at pH 7.4 for 24 h, indicating the excellent stability of the micelles (Fig. S3, ESI[†]).

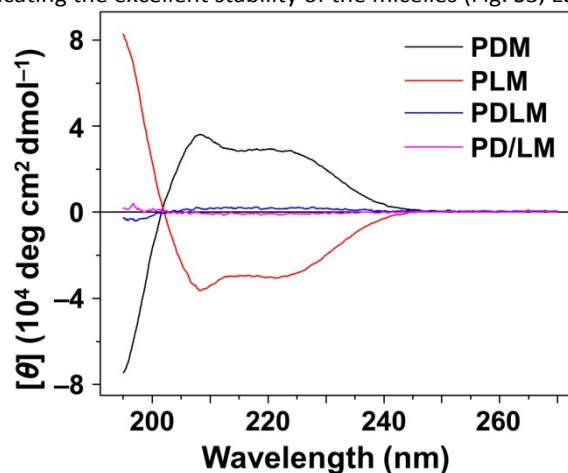


Fig. 2 CD spectra of PDM, PLM, PDLM, and PD/LM at the same concentration of 0.5 mg mL⁻¹.

To reveal the mechanism of adjusting the performances of micelles through changing the secondary structure of PLeu, circular dichroism (CD) spectra of APEG-*b*-PDLeu, APEG-*b*-PLLeu, APEG-*b*-PDLLeu, and equimolar APEG-*b*-PDLeu and APEG-*b*-PLLeu in neutral aqueous condition were recorded to confirm the configuration of PLeu blocks. As depicted in Fig. 2, the CD spectra of PDM and PLM showed double maxima and double minima at 208 and 222 nm, respectively,

demonstrating the formation of almost complete left-handed α -helix in PDM and right-handed α -helix in PLM.^{6, 15} On the contrary, CD signals from PDLM and PD/LM could not be detected because of the mesomeric and racemic PLeu compositions.

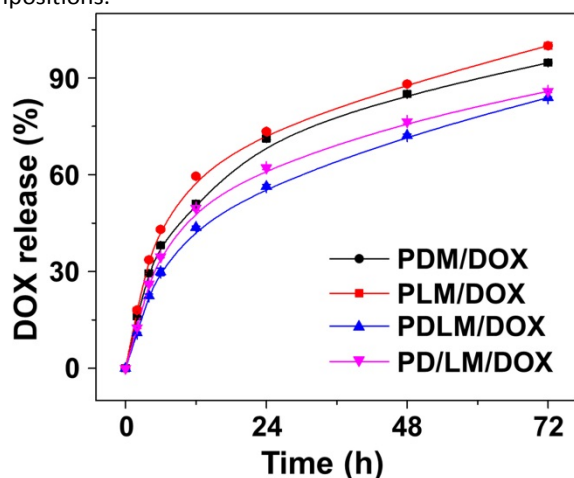


Fig. 3 Release plots of DOX from PDM/DOX, PLM/DOX, PDLM/DOX, and PD/LM/DOX in PBS at pH 7.4, 37 °C.

As shown in Scheme 1, doxorubicin (DOX) was chosen as a model antitumor drug for being encapsulated into micelles through a nanoprecipitation technique to improve the chemotherapy efficacy and decrease the serious side effects.¹⁶ The drug-loaded micelles were noted as PDM/DOX, PLM/DOX, PDLM/DOX, PD/LM/DOX, and R-PDLM/DOX, respectively. As shown in Table S1, ESI[†], the drug loading content (DLC) of PDLM/DOX was 1.5, 2.0, and 1.1 times higher than those of PDM/DOX, PLM/DOX, and PD/LM/DOX, respectively. The DLE values of PDM/DOX, PLM/DOX, PDLM/DOX, and PD/LM/DOX were 17.4, 24.1, 36.0, and 32.5 wt.%, respectively. The highest DLC and DLE of PDLM/DOX should be attributed to a more compact micelle core with hydrophobic mesomeric polypeptide block as mentioned above.

The DOX release behaviors of loading micelles *in vitro* were studied in PBS at pH 7.4, 37 °C (Fig. 3). Both PDM/DOX and PLM/DOX exhibited a quicker DOX release due to a looser micelle core, which was propped up by the rigid polypeptide block, compared with PDLM/DOX and PD/LM/DOX. PDLM/DOX demonstrated the slowest DOX release behavior attributed to the most compact PLeu core with mesomeric structure. In addition, it was noticed that a given mass of encapsulated DOX was not released in 72 h from laden micelles, which should be owing to the enhanced physical interactions, *e.g.*, hydrogen bonding and hydrophobic interactions, between PLeu and DOX.

According to the results of morphology, diameter, and release profile, it could be concluded that the micelle with mesomeric polypeptide as matrix had the best physicochemical property as a nanocarrier for drug delivery. So PDLM/DOX and R-PDLM/DOX were chosen for further research. The endocytosis and intracellular DOX release of drug-loaded micelles toward MDA-MB-231 cells were assessed by both confocal laser scanning microscopy (CLSM) and flow cytometry

(FCM) (Fig. 4). In CLSM and FCM assays, MDA-MB-231 cells were co-cultured with R-PDLM/DOX, PDLM/DOX, or free DOX at an equivalent DOX dose of 2.5 and 5.0 mg L⁻¹, respectively, for 2 h. As shown in Fig. 4A, the highest DOX fluorescence intensity in the nuclear region was observed in the R-PDLM/DOX group compared with those of PDLM/DOX and free DOX groups. The cells co-cultivated with free DOX exhibited lower DOX fluorescence in the nuclei in comparison to those with R-PDLM/DOX because R-PDLM/DOX showed enhanced cellular uptake facilitated by the receptor-mediated endocytosis and sustained intracellular DOX release. As depicted in Fig. 4B, the results of FCM assays verified the results of CLSM assessment shown in Fig. 4A. The intracellular DOX fluorescence intensity was in the following order of R-PDLM/DOX > free DOX > PDLM/DOX after culture for 2 h. The relative geometrical mean fluorescence intensities (GMFIs) were shown in Fig. S4, ESI[†]. The GMFI of R-PDLM/DOX was 1.8 and 1.7 times higher than those of PDLM/DOX and free DOX, respectively. All these results proved that mesomeric PLeu could be commendable hydrophobic polypeptide segment applied for drug delivery, and the targeting effect of cRGD could enhance the selective cellular internalization and might further give upregulated tumor inhibition efficacy.

Subsequently, the *in vitro* cytocompatibility of micelles toward MDA-MB-231 cells in 72 h were assessed by a methyl thiazolyl tetrazolium (MTT) assay. Both R-PDLM and PDLM showed almost no cytotoxicities up to 100.0 mg L⁻¹, revealed by the high cell viability (> 90%) in Fig. S5, ESI[†]. It demonstrated that the micelles revealed unexceptionable cytocompatibility and showed their promising application as nanocarriers for drug delivery.

Moreover, the inhibition efficacies of R-PDLM/DOX and PDLM/DOX against the proliferation of MDA-MB-231 cells in 24 h were further assessed through MTT tests with free DOX as control. From Fig. 5, the inhibition efficacies of DOX-loaded micelles and free DOX toward the proliferation of MDA-MB-231 cells were in the sequence of R-PDLM/DOX > free DOX > PDLM/DOX. Due to the targeting effect of cRGD embedded on the surface of micelle to the $\alpha_v\beta_3$ integrin on the surface of MDA-MB-231 cells, the cytotoxicity of R-PDLM/DOX was higher than those of PDLM/DOX and free DOX. The half maximal inhibitory concentrations (IC₅₀s) of R-PDLM/DOX, PDLM/DOX, and free DOX were 0.11, 1.57, and 0.27 mg L⁻¹, respectively (Table S1, ESI[†]). The result quantitatively confirmed the enhanced antitumor efficacy of R-PDLM/DOX compared with PDLM/DOX and free DOX. The highest cytotoxicity of R-PDLM/DOX should be attributed to its quickest endocytosis through targeting ligand-mediated endocytosis than that of PDLM/DOX and sustained intracellular drug release in comparison with free DOX. All the results demonstrated that the targeting ligand-decorated polypeptide micelle was a promising nanocarrier for directional antitumor drug delivery with upregulated efficacy.

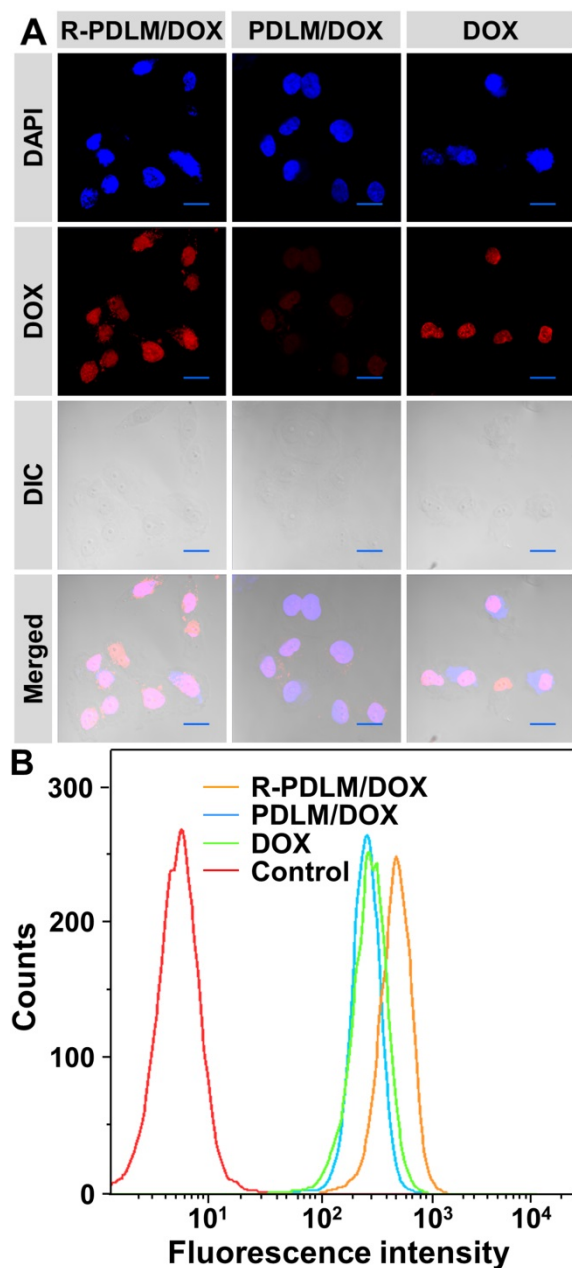


Fig. 4 Typical CLSM micrographs (A) and FCM profiles (B) of MDA-MB-231 cells after incubation with R-PDLM/DOX, PDLM/DOX, or free DOX for 2 h. Scale bar: 20.0 μm .

Conclusions

Four kinds of micelles with hydrophobic dextrorotatory (PDLeu), levorotatory (PLLeu), mesomeric (PDLLeu), and racemic (PDLeu/PLLeu) polypeptide cores were prepared to reveal the influence of polypeptide configurations on the properties of micelles. Among them, PDLM exhibited the most homogeneous size and compact core, which endowed the micelle with the highest drug loading capability. Subsequently, the targeting agent of cRGD, which can identify the $\alpha_v\beta_3$ integrin on the surface of certain tumor cells was conjugated to the terminal of APEG-*b*-PDLLeu by thiol-ene click reaction,

yielding the matrix of targeting micelle, that is, R-PDLM. In addition, R-PDLM/DOX was demonstrated to exhibit enhanced endocytosis and cytotoxicity compared with the untargeted PDLM/DOX and even free DOX. The results revealed that the targeting ligand-decorated mesomeric polypeptide micelle exhibited great potential in controlled drug delivery.

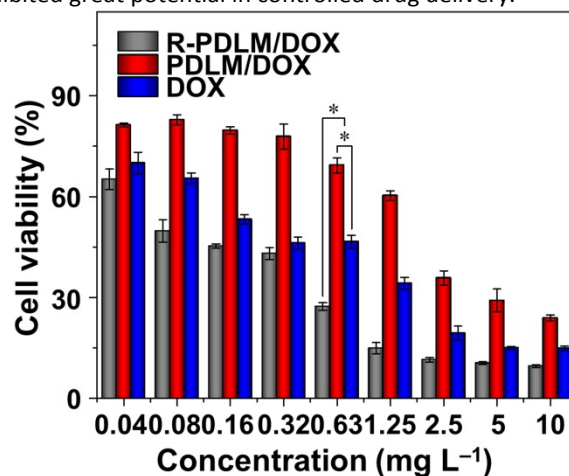


Fig. 5 *In vitro* inhibition efficacies of R-PDLM/DOX and PDLM/DOX with free DOX as control after incubation for 24 h. Data were presented as mean \pm standard deviation ($n = 3$; $*P < 0.001$).

Acknowledgements

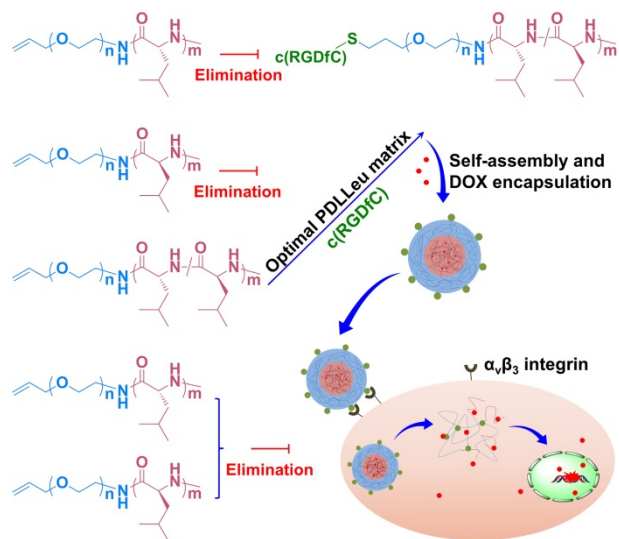
This research was financially supported by National Natural Science Foundation of China (Nos. 51103015, 51303174, 51233004, 51390484, and 51321062), and Scientific Development Program of Jilin Province (Nos. 20140520050JH).

Notes and references

1. H. Lu, J. Wang, Z. Song, L. Yin, Y. Zhang, H. Tang, C. Tu, Y. Lin and J. Cheng, *Chem. Commun.*, 2014, **50**, 139–155.
2. C. Deng, J. Wu, R. Cheng, F. Meng, H.-A. Klok and Z. Zhong, *Prog. Polym. Sci.*, 2014, **39**, 330–364.
3. J. V. González-Aramundiz, M. V. Lozano, A. Sousa-Herves, E. Fernandez-Megia and N. Csaba, *Expert Opin. Drug Del.*, 2012, **9**, 183–201.
4. J. Ding, L. Zhao, D. Li, C. Xiao, X. Zhuang and X. Chen, *Polym. Chem.*, 2013, **4**, 3345–3356.
5. J. Huang and A. Heise, *Chem. Soc. Rev.*, 2013, **42**, 7373–7390.
6. Y. Mochida, H. Cabral, Y. Miura, F. Albertini, S. Fukushima, K. Osada, N. Nishiyama and K. Kataoka, *ACS Nano*, 2014, **8**, 6724–6738.
7. J. Ding, C. Li, Y. Zhang, W. Xu, J. Wang and X. Chen, *Acta Biomater.*, 2015, **11**, 346–355.
8. S. Hehir and N. R. Cameron, *Polym. Int.*, 2014, **63**, 943–954.
9. S. Quader, H. Cabral, Y. Mochida, T. Ishii, X. Liu, K. Toh, H. Kinoh, Y. Miura, N. Nishiyama and K. Kataoka, *J. Control. Release*, 2014, **188**, 67–77.
10. J. A. Hanson, Z. Li and T. J. Deming, *Macromolecules*, 2010, **43**, 6268–6269.
11. P. F. Gu, H. Xu, B. W. Sui, J. X. Gou, L. K. Meng, F. Sun, X. J.

- Wang, N. Qi, Y. Zhang, H. B. He and X. Tang, *Int. J. Nanomed.*, 2012, **7**, 109–122.
12. J. W. Kim, F. V. Cochran and J. R. Cochran, *J. Am. Chem. Soc.*, 2015, **137**, 6–9.
13. Y. Shen, X. Fu, W. Fu and Z. Li, *Chem. Soc. Rev.*, 2015, **44**, 612–622.
14. J. Ding, J. Chen, D. Li, C. Xiao, J. Zhang, C. He, X. Zhuang and X. Chen, *J. Mater. Chem. B*, 2013, **1**, 69–81.
15. J. Ding, C. Xiao, L. Zhao, Y. Cheng, L. Ma, Z. Tang, X. Zhuang and X. Chen, *J. Polym. Sci. Part A: Polym. Chem.*, 2011, **49**, 2665–2676.
16. H. Cabral and K. Kataoka, *J. Control. Release*, 2014, **190**, 465–476.

TOC Graphic



TOC text

The mesomeric poly(2-oxazoline) micelle with cRGD decoration is screened out for promising targeting drug delivery.